International Journal of Nanomedicine

Dovepress
open access to scientific and medical research

Open Access Full Text Article

ORIGINAL RESEARCH

Formulation, characterization, and evaluation of in vitro skin permeation and in vivo pharmacodynamics of surface-charged tripterine-loaded nanostructured lipid carriers

This article was published in the following Dove Press journal:
International Journal of Nanomedicine
20 June 2012
Number of times this article has been viewed

Yan Chen
Lei Zhou
Ling Yuan
Zhen-hai Zhang
Xuan Liu
Qingqing Wu

Key Laboratory of New Drug Delivery System of Chinese Materia Medica, Jiangsu Provincial Academy of Chinese Medicine, Nanjing, Jiangsu, China

Background: Nanostructured lipid carriers (NLCs) are attractive materials for topical drug delivery, and in a previous study, we demonstrated that NLCs loaded with tripterine enhance its deposition. However, the surface charge of nanoparticles influences percutaneous drug penetration. Therefore, we aimed to evaluate the influence of the surface charge of NLCs on in vitro skin permeation and in vivo pharmacodynamics of tripterine and optimize tripterine-loaded NLCs for the treatment of skin diseases.

Methods: Different solid and liquid matrices were selected to prepare cationic, anionic, and neutral NLCs by the solvent evaporation method. The in vitro studies were evaluated by using Franz diffusion cells. The effect of surface-charged NLCs on cellular uptake was appraised across HaCaT and B16BL6 cells. The in vitro and in vivo anticancer activity of surface-charged NLCs was evaluated in B16BL6 cells and melanoma-bearing mice, respectively.

Results: The average particle sizes of the cationic, anionic, and neutral NLCs were 90.2 ± 9.7, 87.8 ± 7.4, and 84.5 ± 10.2 nm, respectively; their encapsulation efficiencies were 64.3% ± 5.1%, 67.8% ± 4.4%, and 72.5% ± 4.9%, respectively. In vitro studies showed delayed tripterine release, and the order of skin permeation was cationic NLCs > anionic NLCs > neutral NLCs. Further, in vitro cytotoxicity studies showed that the cationic NLCs had the highest ($P < 0.05$) inhibition ratio in B16BL6 (melanoma) cells. Moreover, in vivo pharmacodynamic experiments in melanoma-bearing mice indicated that the cationic NLCs had significantly higher ($P < 0.05$) antimelanoma efficacy than the anionic and neutral NLCs.

Conclusion: The surface charge of NLCs has a great influence on the skin permeation and pharmacodynamics of tripterine. Cationic tripterine-loaded NLCs could enhance the percutaneous penetration and antimelanoma efficacy of tripterine and offer several advantages over tripterine alone. Therefore, they are promising carriers of tripterine for topical antimelanoma therapy.

Keywords: surface charge, nanostructured lipid carriers, tripterine, percutaneous penetration, cellular uptake, antimelanoma efficacy

Introduction

Nanostructured lipid carriers (NLCs) are regarded as an alternative to liposomes and nanoemulsions, due to various advantages, such as ease of manufacture, particulate nature, high drug loading, and sustained drug release.[1] Their biocompatibility, modified release kinetics, easy large-scale production, and limited drug leakage during storage indicate that they are suitable for topical drug delivery.[2,3] Topical delivery offers several advantages over the oral and intravenous dosage routes, such as prevention of first-pass metabolism, minimization of pain, and possible controlled release of drugs.[4,5]

Correspondence: Yan Chen
Key Laboratory of New Drug Delivery System of Chinese Materia Medica, Jiangsu Provincial Academy of Chinese Medicine, 100 Shizi Road, Nanjing, Jiangsu 210028, People's Republic of China
Tel +86 25 85608672
Fax +86 25 85637809
Email ychen202@yahoo.com.cn

submit your manuscript | www.dovepress.com
Dovepress
http://dx.doi.org/10.2147/IJN.S32476

Tripterine, a bioactive compound identified in the traditional Chinese medicinal plant *Tripterygium wilfordii* Hoog f. almost three decades ago, is generally used for the treatment of inflammatory and autoimmune diseases.[6] It has attracted great interest recently because of its potential anti-inflammatory and anticancer activities, as well as its therapeutic applicability for skin diseases.[7–9] However, tripterine has low bioavailability, due to its negligible water solubility. It also causes many severe adverse effects when administered orally, such as diarrhea, headache, nausea, and infertility.[10]

To overcome these disadvantages, in a previous study, we prepared tripterine-loaded NLCs, and we found that they enhance the deposition and in vitro skin permeation of tripterine.[11] However, many researchers have indicated that the surface charge of nanoparticles influences percutaneous drug penetration.[12] For example, Song and Kim[13] showed that the in vitro skin permeation of low-molecular-weight heparin and its in vivo penetration into the deeper skin layers are significantly better from cationic flexible liposomes than from anionic and neutral flexible liposomes.

Therefore, we aimed to evaluate the influence of the surface charge of NLCs on in vitro skin permeation and in vivo pharmacodynamics of tripterine, as well as to optimize tripterine-loaded NLCs for the treatment of skin diseases. We selected different solid and liquid matrices to prepare cationic, anionic, and neutral NLCs. The in vitro skin permeation, in vitro cytotoxicity, and in vivo pharmacodynamics were investigated by using Franz diffusion cells, B16BL6 cells, and melanoma-bearing C57BL/6 mice, respectively. The results indicate that these surface-charged NLCs have good encapsulation efficiency and favorable physicochemical characteristics. These formulations, especially cationic ones, considerably increase the deposition and antimelanoma efficacy of tripterine. Herein, we show that cationic NLCs are promising carriers of tripterine for topical antimelanoma therapy.

Materials and methods

Materials

Tripterine (>99.9% purity) was provided by Nanjing Zelang Medical Technology Co, Ltd (Nanjing, Jiangsu, China). Glyceryl behenate, isopropyl myristate (IPM), Pluronic F68, acetone, and ethanol were obtained from Shanghai Chemical Reagent Corp (Shanghai, China). Precirol ATO-5, medium-chain triglycerides (MCTs), and stearylamine were purchased from Gattefossé (Saint-Priest, Lyon, France). Soybean lecithin was supplied by Shanghai Advanced Vehicle Technology Co (Shanghai, China). D-α-Tocopherol polyethylene glycol succinate was purchased from Sigma-Aldrich Shanghai Trading Co, Ltd (Shanghai, China). All reagents were of analytical or high-performance liquid chromatography (HPLC) grade. Double-distilled water was prepared in our laboratory.

Animals and cell lines

Male Sprague–Dawley rats (200–230 g) and male C57BL/6 mice (18–20 g) were obtained from the Shanghai Laboratory Animal Center (Shanghai, China). The animal experiment protocol was reviewed and approved by the Institutional Animal Care and Use Committee of Jiangsu Provincial Academy of Chinese Medicine (SCXK 2012-0005).

HaCaT (normal human skin) cells and B16BL6 (melanoma) cells were purchased from Nanjing KeyGen Biotech Co, Ltd (Nanjing, China).

Preparation of NLCs

Blank NLCs were prepared by the solvent evaporation method. The proportion of solid and liquid matrices was set to 3:1 wt%. Soybean lecithin and D-α-tocopherol polyethylene glycol succinate were used as emulsifiers. Each formulation was dissolved in a mixture of acetone and ethanol and added to an aqueous surfactant solution containing Pluronic F68 (1.0 wt%) at 65°C, under gentle magnetic stirring, at 400 rpm for 4 hours. An external water bath (0°C–2°C) was used to maintain the sample temperature for 2 hours to stabilize the NLCs. The total volume of the final product was 25 mL. The resultant NLC dispersions were used for the subsequent studies. NLCs containing 15 mg tripterine were similarly prepared to obtain tripterine-loaded NLCs.

In preliminary experiments, stearylamine, glyceryl behenate, and Precirol ATO-5 were chosen as the solid matrix for cationic, neutral, and anionic NLCs, respectively. MCT was chosen as the liquid matrix for neutral NLCs, and IPM was chosen as the liquid matrix for cationic and anionic NLCs. The composition of the surface-charged NLC dispersions is presented in Table 1.

Photon correlation spectroscopy

The particle size and polydispersity index (PI) of the NLC formulations were measured by photon correlation spectroscopy (Zetasizer Nano ZS ZEN3600; Malvern Instruments Ltd, Worcestershire, UK) at 25°C, under a fixed angle of 90°, in polystyrene cuvettes. The measurements were obtained by using a 633 nm He–Ne laser.

The zeta potential was measured in folded capillary cells by using the Zetasizer. NLC samples were prepared by dilution with double-distilled water. The conductivity of

Table 1 Composition of the surface-charged NLCs

Formulation	Stearylamine (mg)	Gb (mg)	Precirol ATO-5 (mg)	IPM (mg)	MCTs (mg)	SLT (mg)	TPGS (mg)
Cationic NLCs	180	–	–	60	–	30	30
Neutral NLCs	–	180	–	–	60	30	30
Anionic NLCs	–	–	180	60	–	30	30

Abbreviations: NLCs, nanostructured lipid carriers; Gb, glyceryl behenate; IPM, isopropyl myristate; MCTs, medium-chain triglycerides; SLT, soybean lecithin; TPGS, D-α-tocopherol polyethylene glycol succinate.

each sample was adjusted to 50 S/cm, by using 0.1 mmol/L sodium chloride solution. The zeta potential values were calculated by using the Smoluchowski equation.[14]

Entrapment efficiency

Ultrafiltration was used to assay entrapment efficiency (EE). In brief, approximately 0.5 mL of NLC dispersion was placed in the upper chamber of a centrifuge tube matched with an ultrafilter (MWCO12 kDa; Pall Corp, Port Washington, NY). The filter assembly was then centrifuged at 5000 rpm (~3000 *g*) for 15 minutes. Surface-charged NLCs, along with encapsulated tripterine, remained in the upper chamber, whereas the aqueous dispersion medium containing free unloaded tripterine was moved to the sample recovery chamber through the filter membrane. After separation, the amount of free tripterine in methanol (W_{free}) was determined by HPLC. Further, an equal volume of tripterine-loaded NLC dispersion was dissolved and diluted with methanol. Then, the total tripterine content in the resultant solution (W_{total}) was determined by HPLC. Finally, the EE was calculated, using the following equation:[15]

$$EE\ (\%) = \frac{W_{total} - W_{free}}{W_{total}} \times 100 \quad (1)$$

The HPLC system (Agilent Technologies, Santa Clara, CA) included a binary pump, an autosampler, and a photodiode array detector. An Agilent HC-C18 column (150 × 4.6 mm inner diameter, 5 µm particle size) was used as the stationary phase. The mobile phase was an acetonitrile–0.4% phosphoric acid (80:20, v/v) mixture at a flow rate of 1 mL/minute, and the injection volume was 20 µL. The detection wavelength was 425 nm (for tripterine). Quantification was based on the peak area A. Linearity was observed over the concentration range of 10–8000 ng/mL, with correlation coefficients of over 0.99 (a typical calibration curve: A = 45.299C + 15.533, r = 0.9999, n = 3). Accuracy for the determination of tripterine (n = 6) was 99.93% ± 1.44%. Intra- and interday precisions were below 2%, and the extraction recovery of tripterine in NLC (n = 9) was 99.52% ± 0.81%.

Transmission electron microscopy

The morphology and lamellarity of the NLCs were examined by transmission electron microscopy (TEM) (Tecnai 12; Royal Philips Electronics, Amsterdam, Netherlands) with the negative stain method. NLC samples were first diluted with double distilled water. A drop of each sample was applied to a copper grid coated with carbon film and air-dried; then, 2% (w/v) phosphotungstic acid (PTA) solution was dropped onto the grids. After negative staining and air-drying at room temperature, the resultant samples were used for visualization under TEM.

Differential scanning calorimetry (DSC)

The broad water peak (~100°C) in DSC may largely influence the judgment of thermograms of lipid nanoparticles. To avoid this interference, NLC samples were freeze-dried before the measurements.[16] About 10 mg of each sample were analyzed in a DSC 204 system (Netzsch, Selb, Germany), and an empty pan was used as the reference. A scan rate of 10°C/minute was employed, in a temperature range of 25°C–300°C. The measurements of each formulation were repeated three times.

Tripterine release kinetics

Release of tripterine from the NLCs was measured by using Franz diffusion cells. Dialysis tubing (molecular weight cut-off of 8,000 to 14,000) was mounted between the donor and the receptor compartments. The donor medium consisted of 2 mL of vehicle containing different surface-charged NLCs, and the receptor medium comprised a 2:8 ratio of ethanol and phosphate-buffered saline (PBS; pH 7.4), to maintain the sink conditions. The stirring rate and temperature were 400 rpm and 37°C, respectively. At various intervals (1, 2, 4, 8, 10, 12, 18, 24, 36, and 48 hours), 1.0 mL aliquots of the receptor medium were removed and immediately replaced with the same volumes of fresh medium. The percentage of tripterine released in the aliquots was calculated with the following equation:

$$\text{Release of tripterine}\ (\%) = \frac{\text{Release tripterine}}{\text{Total tripterine used}} \times 100 \quad (2)$$

Skin permeation experiment

The skin permeation of tripterine from the surface-charged NLCs was measured by using a Franz diffusion assembly. The full-thickness abdominal skin of young male Sprague–Dawley rats was mounted between the donor and receptor compartments. The exposed skin surface area was 2.00 cm^2, and the receptor compartment volume was 20 mL. The donor medium consisted of 1 mL of tripterine-containing vehicle, and the receptor medium was a 3:7 ratio of ethanol and PBS (pH 7.4), to maintain the sink conditions. The stirring rate and temperature were 600 rpm and 37°C, respectively. At appropriate intervals (1, 2, 4, 6, 8, 10, and 12 hours), 1 mL aliquots of the receptor medium were withdrawn and immediately replaced with equal volumes of fresh medium. After the experiment, the skin was frozen at −20°C on a metal sample holder and sectioned with a cryotome (620 Electronic; Thermo-Shandon, Pittsburgh, PA) in layers of 0–30, 30–60, and 60–90 μm thickness. The amount of tripterine in each layer was determined by HPLC. The cumulative amount of tripterine permeating through the skin was plotted as a function of time. Data analyses of cumulative amounts of tripterine permeated over time were used to calculate the transdermal drug flux, which was obtained from the slope of the regression line, fitted to the linear portion of the profile. The skin flux can be experimentally determined from the following equation:

$$J = (dQ/dt)/A \quad (3)$$

where J is the steady-state flux (μg/($cm^2 \cdot h$)), A is the diffusion area of skin tissue (cm^2) through which drug permeation takes place, and dQ/dt is the amount of drug passing through the skin per unit time at a steady-state (μg/h). The intercept of the extrapolated linear region with the x-axis provided the lag time. The following equation was used to calculate the permeability coefficient (Kp):

$$Kp = J/Co \quad (4)$$

where Kp has the units of cm/h, and Co represents the drug concentration.

MTT assay

For cytotoxicity analysis, B16BL6 cells were seeded at 9×10^3 cells/well in 96-well plates and incubated at 37°C and 5% CO_2 for 24 hours. After overnight incubation, the cells were divided into four treatment groups: (i) tripterine solution group; (ii) cationic NLC group; (iii) neutral NLC group; and (iv) anionic NLC group. They were treated with various concentrations (2–10 μg/mL; 0 μg/mL was the negative control) of tripterine and tripterine-loaded NLCs for 36 hours. Then, 10 μL of 3-(4,5-dimethylthiazol-2-yl)-2,5-diphenyltetrazolium bromide (MTT; 5 mg/mL) was added to each well and incubated for 4 hours at 37°C. After the supernatant was discarded, 100 μL dimethyl sulfoxide was added to each well. The absorbance value at 550 nm was determined by using a microplate reader (Thermo Fisher Scientific, Waltham, MA). Any interference of the absorbance readings by particle fluorescence was monitored and accounted for.

Evaluation of cellular uptake

Cellular uptake of nanoparticles, including NLCs, by various cell types has been described in the literature already and could be clinically relevant when applied to the skin. To determine cellular uptake of tripterine, 12 mL of each NLC formulation (5 μg/mL) was added to HaCaT and B16BL6 cells. After incubation for up to 4 hours, the cells were washed three times with PBS (pH 7.2) and lysed in an ultrasonic cell pulverizer (JY92-IIN; Xinzhi Co, China). The amount of tripterine in the cell lysate (W_{in}) was quantified by HPLC, and the percentage of cellular uptake was calculated with the following equation:

$$\text{Cellular uptake (\%)} = \frac{W_{in}}{W_{total}} \times 100 \quad (5)$$

Pharmacodynamic evaluation

B16BL6 cells were maintained in Roswell Park Memorial Institute 1640 medium, supplemented with 10% fetal bovine serum and antibiotics. They were then trypsinized, resuspended in PBS (2×10^7 cells/mL), and subcutaneously injected into the nota of male C57BL/6 mice. The mice were randomly divided into various groups (n = 10/group) according to the treatment: control, tripterine solution, cationic NLCs, neutral NLCs, and anionic NLCs. These treatments were administered by percutaneous penetration daily. In the tripterine-based treatments, 6 mg/kg of tripterine in 1% carbomer gel was used. As the positive control, cyclophosphamide (CTX, 20 mg/kg) was administered daily by intraperitoneal injection. After 16 consecutive days, the tumors were excised and weighed.[17]

Statistical analysis

Data are expressed as means ± standard deviation (SD). One-way analysis of variance (ANOVA) in IBM SPSS 11.5 software (IBM, Armonk, NY) was used for multiple comparisons, and unpaired Student's *t*-test in Microsoft Excel was used to compare two groups. The level of significance was set at $P < 0.05$.

Results

Particle size, PI, zeta potential, and EE

Table 2 shows the results obtained by photon correlation spectroscopy and ultrafiltration. The particle size of the surface-charged NLCs ranged from 84.5 ± 10.2 to 90.2 ± 9.7 nm, without significant differences among these formulations. Their PIs ranged from 0.109 ± 0.018 to 0.116 ± 0.024. The zeta potential values of the cationic and anionic NLCs were 26.4 ± 4.2 and −24.3 ± 3.7 mV, respectively. The neutral NLCs had a small negative surface charge (−2.7 ± 0.9 mV).

As shown in Table 2, the EE values of the formulations ranged from 67.8% ± 4.4% to 72.5% ± 4.9%.

Morphology and lamellarity

The TEM results are shown in Figure 1. The particles had a spherical shape, with a smooth surface. The different NLCs showed no marked structural differences.

Melting behavior and crystallinity

DSC is used to characterize the melting and crystallization behaviors of crystalline materials, such as lipid nanoparticles.[18,19] In the case of NLCs, DSC can clarify their structure through the mixing behavior of solid lipids with liquid lipids. Figure 2 shows the DSC curves of the surface-charged NLCs. Tripterine alone exhibited melting peaks at around 175.7°C and 211.4°C. Furthermore, the physical mixture with tripterine showed a melting point at 211.4°C. In the DSC curves of physical mixtures I and physical mixtures II regarding cationic NLCs, the peak of lipid material was transferred from 68.3°C to 78.2°C, and from 89.4°C to 81.5°C. The same phenomenon was observed with the neutral and anionic NLCs, which were produced in the initial equilibrium process, because of the slightly different temperatures between the sample and the reference pans. Comparing Figure 2A–C, the same state of tripterine in the different surface charged NLCs can be seen. Tripterine was in the amorphous state in the surface-charged NLCs, as reported previously by Gonzalez-Mira.[20]

Table 2 Physical properties of the surface-charged NLCs

Formulation	Size (nm)	Zeta potential (mV)	PI	EE (%)
Cationic NLCs	90.2 ± 9.7	26.4 ± 4.2	0.109 ± 0.018	69.3 ± 5.1
Neutral NLCs	87.8 ± 7.4	−2.7 ± 0.9	0.113 ± 0.029	67.8 ± 4.4
Anionic NLCs	84.5 ± 10.2	−24.3 ± 3.7	0.116 ± 0.024	72.5 ± 4.9

Note: Data represent means ± SD (n = 3).
Abbreviations: NLCs, nanostructured lipid carriers; PI, polydispersity index; EE, entrapment efficiency.

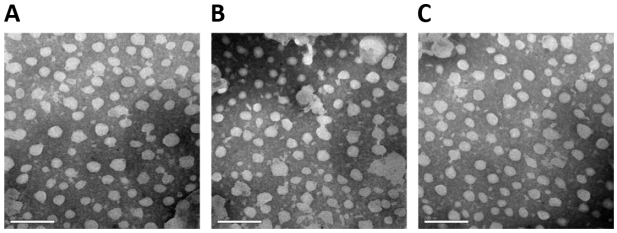

Figure 1 Transmission electron microscopy images of the surface-charged tripterine-loaded nanostructured lipid carriers (NLCs). (**A**) Cationic NLCs; (**B**) neutral NLCs; and (**C**) anionic NLCs.

Tripterine release

The percentage of tripterine released from each NLC formulation was plotted as a function of time (Figure 3). In the initial 18 hours, the cationic, neutral, and anionic NLCs released 36.70%, 39.09%, and 31.94% of tripterine, respectively, without significant differences among the NLCs. After 24 hours, the release was 64.77%, 75.69%, and 49.70%, respectively; at the end of 48 hours, the percentage of released tripterine reached 83.14%, 95.15%, and 68.01%, respectively.

The release profiles of tripterine from the NLCs were fitted into zero-order, first-order, Higuchi, and Ritger and Peppas kinetic models (Table 3).[21] The first-order kinetic model was chosen to describe the release profiles because of good correlation. The r^2 values for the cationic, neutral, and anionic NLCs were 0.9559, 0.9521, and 0.9614, respectively.

Skin permeation

Figure 4 and Table 4 illustrate the in vitro skin permeation of tripterine from the different formulations. The cumulative penetration of tripterine was significantly different ($P < 0.05$) among the cationic, neutral, and anionic NLCs (16.3 ± 0.81, 13.5 ± 0.79, and 11.9 ± 0.85 μg/cm^2, respectively; Figure 4A). The flux of the cationic, neutral, and anionic NLCs was

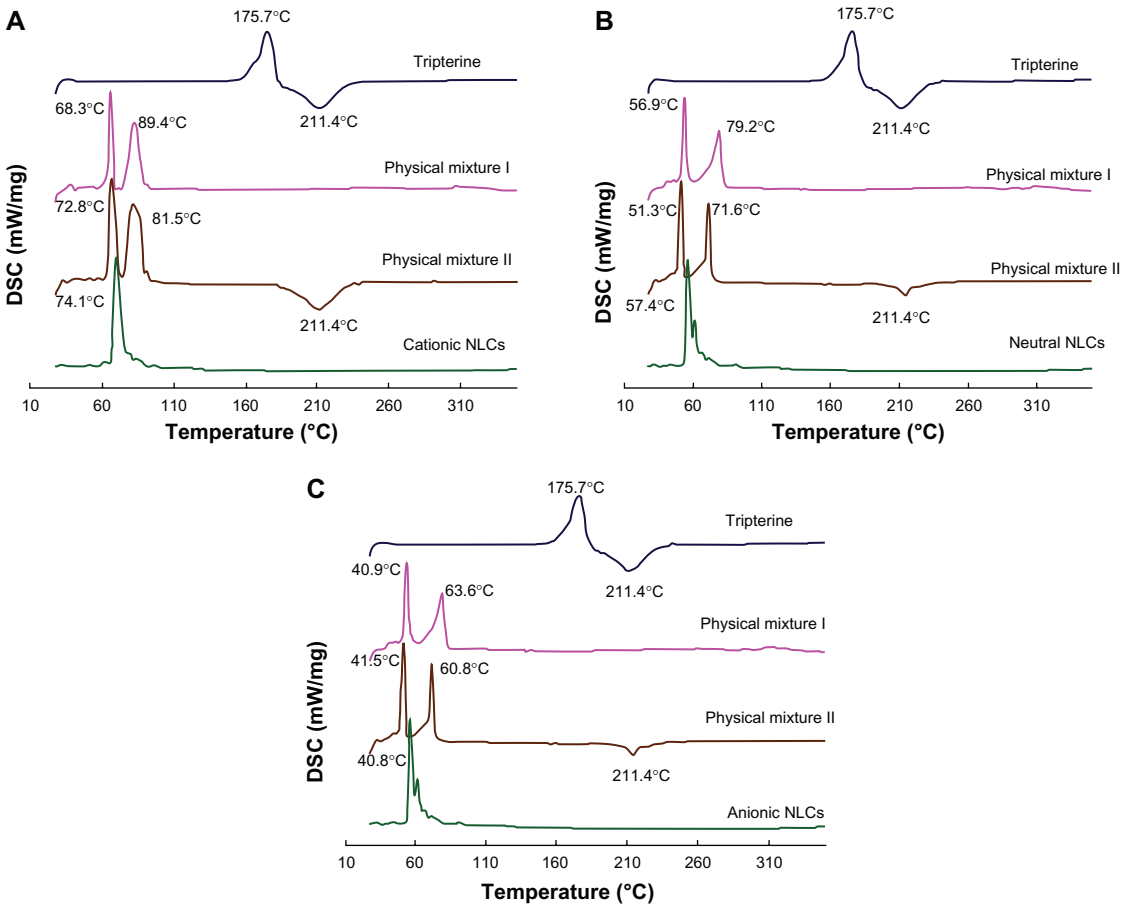

Figure 2 DSC curves of the surface-charged tripterine-loaded NLCs. (**A**) Cationic NLCs; (**B**) neutral NLCs; and (**C**) anionic NLCs. Curves of tripterine and physical mixtures with (mixture II) and without (mixture I) tripterine are also shown.
Abbreviations: DSC, differential scanning calorimetry; NLCs, nanostructured lipid carriers.

1.26 ± 0.29, 1.10 ± 0.25, 0.91 ± 0.04 μg/(cm^2 · h), respectively (Figure 4A and Table 4). Cationic NLCs increased the tripterine permeability coefficient 1.15- and 1.38-fold compared to that of neutral and anionic NLCs, respectively (Figure 4A and Table 4). The skin deposition of tripterine decreased in the following order: 0–30 μm > 30–60 μm > 60–90 μm (Figure 4B). The cationic NLCs delivered 10.6 μg/cm^2 of tripterine into the skin, which was 1.35- and 1.95-fold higher ($P < 0.05$) than the amounts provided by the neutral and anionic NLCs, respectively.

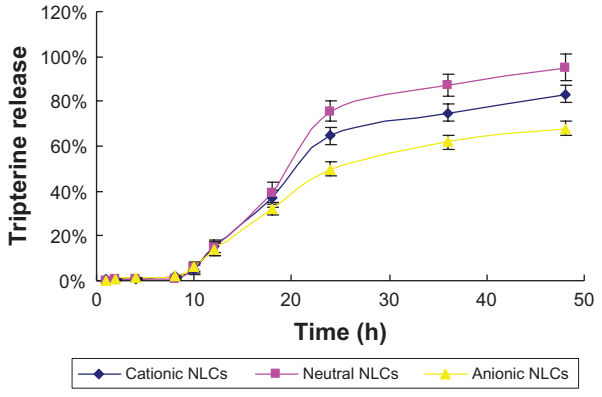

Figure 3 Time course of tripterine release from the surface-charged nanostructured lipid carriers (NLCs).
Note: Data represent means ± SD (n = 3).

Cytotoxicity

The inhibition ratio and half-maximal inhibitory concentration (IC_{50}) of the surface-charged NLCs in B16BL6 cells are shown in Table 5. At the same concentrations, the cationic NLCs had higher cell inhibition ratios than the neutral and anionic NLCs. Further, the cationic NLCs had a better IC_{50} value.

Cellular uptake

The uptake of tripterine from the surface-charged NLCs by HaCaT and B16BL6 cells is shown in Figure 5. After 1, 2, 3, and 4 hours of incubation, 20.1%, 27.6%, 36.4%, and 44.6% of tripterine, respectively, from the cationic NLCs were measured in HaCaT cells. At the same time points, 16.8%,

Table 3 Fitting of the accumulated release data

Equation	Cationic NLCs	Neutral NLCs	Anionic NLCs
Zero order	$Q = 0.0208t - 0.0546$; $r^2 = 0.9199$	$Q = 0.0242t - 0.0755$; $r^2 = 0.9131$	$Q = 0.0169t - 0.0406$; $r^2 = 0.9347$
First order	$\ln(1 - Q) = -0.0418t + 0.1891$; $r^2 = 0.9559$	$\ln(1 - Q) = -0.0678t + 0.3084$; $r^2 = 0.9521$	$\ln(1 - Q) = -0.0275t + 0.1051$; $r^2 = 0.9614$
Higuchi	$Q = 0.1638t - 0.3042$; $r^2 = 0.8887$	$Q = 0.1904t - 0.3646$; $r^2 = 0.8775$	$Q = 0.1336t - 0.2449$; $r^2 = 0.9077$
Ritger and Peppas	$\ln Q = 1.4908\ln t - 5.8389$; $r^2 = 0.8981$	$\ln Q = 1.8519\ln t - 6.9165$; $r^2 = 0.9149$	$\ln Q = 1.691\ln t - 6.5524$; $r^2 = 0.9551$

Abbreviations: NLCs, nanostructured lipid carriers; Q, the percentage of released tripterine.

22.5%, 30.6%, and 37.8%, respectively, of tripterine from the neutral NLCs and 13.4%, 21.3%, 29.5%, and 35.1% of tripterine, respectively, from the anionic NLCs were measured (Figure 5A).

Similar results were obtained in B16BL6 cells. The cellular uptake of tripterine decreased in the following order: cationic NLCs > neutral NLCs > anionic NLCs. As shown in Figure 5C, after different incubation times, the uptake of tripterine from the cationic NLCs was higher in B16BL6 cells than in HaCaT cells.

Effects on tumor growth

As shown in Figure 6A, the tumor volume in the tripterine, tripterine-loaded NLC, and CTX groups was visibly smaller than in the control group. The order of tumor weight was control group > tripterine group > cationic NLC group > neutral NLC group > anionic NLC group > CTX group (Figure 6B). The tumor inhibition rate of the cationic NLCs was 50.58%, whereas those of the neutral NLCs, anionic NLCs, and tripterine were 43.02%, 38.95%, and 29.65%, respectively, on the 16th day (Figure 6C).

Discussion

In this study, we investigated the influence of the surface charge of tripterine-loaded NLCs on the in vitro skin permeation and in vivo pharmacodynamics of the drug. We found that the surface charge greatly affects these properties. Specifically, higher tripterine deposition and antimelanoma efficacy were achieved with cationic NLCs.

Particle size, PI, and zeta potential are important properties associated with the stability and acceptability of a topical drug delivery system. The surface-charged NLCs had a mean particle size smaller than 100 nm. Small particle size is a highly desirable property of NLCs, because the penetration of encapsulated drugs into deeper skin layers increases with decrease in particle size.[15] The PI of the NLCs was lower than 0.2, indicating their satisfactory homogeneity and suitability for topical drug delivery. Regarding the zeta potential, the NLCs possessed only a small negative surface charge and, therefore, were considered neutral NLCs. The cationic NLCs possessed a high positive surface charge, whereas the anionic NLCs possessed a high negative surface charge. However, their absolute zeta potential values were almost the same. Stearylamine and Precirol ATO-5

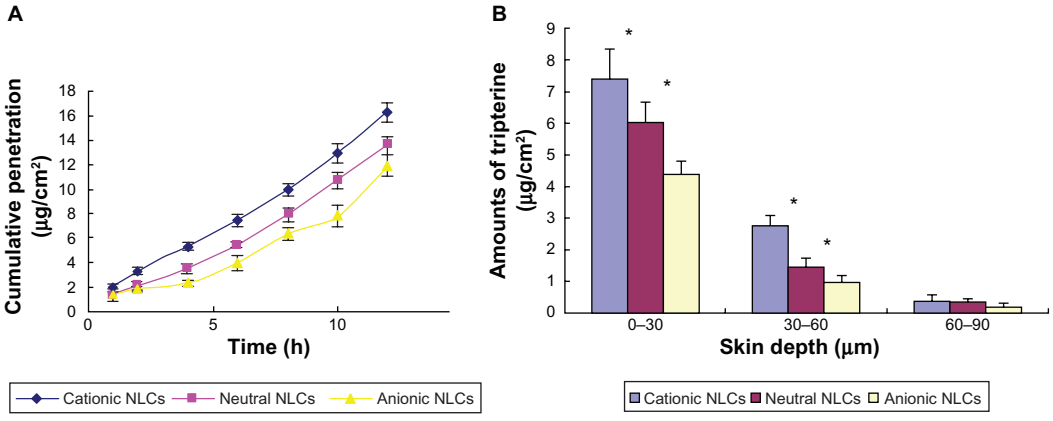

Figure 4 In vitro skin permeation of tripterine from the surface-charged tripterine-loaded NLCs 12 hours after their application on rat abdominal skin. (**A**) Time course of cumulative penetration and (**B**) amounts of tripterine in different layers of skin.
Notes: Data represent means ± SD (n = 3); *$P < 0.05$ versus the anionic NLCs.
Abbreviation: NLCs, nanostructured lipid carriers.

Table 4 The flux (μg/(cm^2 · h)) and permeability coefficient of tripterine across rat skin

Formulation	Flux (μg/(cm^2 · h))	Lag time (h)	Permeability coefficient (cm/h) × 10^{-3}
Cationic NLCs	1.26 ± 0.29*	0.43 ± 0.02*	2.10 ± 0.49*
Neutral NLCs	1.10 ± 0.25	0.42 ± 0.05	1.83 ± 0.43
Anionic NLCs	0.91 ± 0.04	0.52 ± 0.02	1.52 ± 0.06

Notes: Data represent means ± SD (n = 3); *$P < 0.05$ versus the anionic NLCs.
Abbreviation: NLCs, nanostructured lipid carriers.

were mixed with IPM in the same ratio to obtain NLCs with similar absolute zeta potential value but opposite charge.

With regard to the EE, the observed greater entrapment of tripterine by the NLCs might be attributable to the liquid state of MCT and IPM, which help to encapsulate larger amounts of lipophilic drugs and reduce particle crystallinity, thus improving stability and suitability for controlled drug release. These results indicated that there was no direct relationship between the lipid phase composition of the NLCs and their EE. Therefore, the effect of the surface charge of the NLCs on the penetration of tripterine could be investigated.

The in vitro release study showed that the surface-charged NLCs released tripterine in a controlled manner, possibly because of the effects of tripterine diffusion and lipid matrix erosion. Tripterine must diffuse from the liquid inner phase to the solid outer surface of the NLCs before it can diffuse from the outer lipid phase into the bulk aqueous phase. Patlolla et al[22] noted similar findings: in their study, nanoparticles prepared with Miglyol oil showed slower celecoxib release, because of the distribution of celecoxib in the inner area of the lipid matrix and longer diffusion path length.

Tripterine generally penetrates the skin poorly, due to its large relative molecular mass and extremely high hydrophobicity. Therefore, topical tripterine formulations are not available on the market. The strategy of using NLCs to overcome the difficulty related to low skin penetration of drugs is gaining interest. We found that the cumulative penetration of tripterine was the greatest from the cationic NLCs. The skin depth profile of tripterine was almost the same as its cumulative penetration profile: the cationic NLCs provided the highest accumulation of tripterine in the deeper skin layers, followed by the neutral and anionic NLCs. These results are in agreement with those of the skin permeation of drugs incorporated in positively charged nanoparticles.[23] They suggest that the skin is a negatively charged membrane, and that the electrostatic interaction between the negatively charged skin surface and the positively charged NLCs could improve drug penetration. Therefore, cationic NLCs could increase the accumulation of tripterine in the skin layers, and the skin layers could act as a reservoir for the drug, which is useful for treating localized diseases.

The in vitro cytotoxicity of drug-loaded nanoparticles is related to both the materials used and the particle size.[24] We used lipids with good biocompatibility, and the different surface-charged NLCs had similarly sized particles. Interestingly, these NLCs showed different cell inhibitory effects at the same concentration; the cationic NLCs had the highest inhibitory effect. The results indicate that the cell inhibition ratio is associated with the surface charge of NLCs. The reason for the high inhibition ratio of the cationic NLCs could be that the positively charged particles have high binding affinity toward the negatively charged B16BL6 cell membrane.

After incubation, the cationic NLCs provided the greatest amount of tripterine in HaCaT and B16BL6 cells, followed by the neutral and anionic NLCs. The increased cellular uptake of tripterine-loaded cationic NLCs could be explained by the presence of the positive charge, which would have high binding affinity toward cell surfaces.[25] The results of cellular uptake could also explain the high skin permeation and inhibition ratio of the cationic NLCs. In addition, B16BL6 cells have a higher negative charge than HaCaT cells, resulting in the higher cellular uptake of the cationic NLCs. These results suggest that cationic NLCs could be a targeting carrier of anticancer drugs.

The pharmacodynamic evaluation clearly demonstrated that all the surface-charged NLCs were significantly more effective than tripterine alone, indicating the advantage of NLCs for tripterine delivery. The reasons for the low

Table 5 Cytotoxic effects of the surface-charged tripterine-loaded NLCs on B16BL6 cells

Formulation	Cell inhibition ratio (%)					IC_{50} (μg/mL)
	2 μg/mL	4 μg/mL	6 μg/mL	8 μg/mL	10 μg/mL	
Cationic NLCs	9.93 ± 0.93	23.36 ± 2.08	48.76 ± 2.15	69.31 ± 1.87	89.10 ± 4.92	5.43
Neutral NLCs	9.06 ± 1.21	21.74 ± 3.12	43.80 ± 2.58	67.66 ± 3.19	86.38 ± 4.03	5.76
Anionic NLCs	8.57 ± 0.89	19.91 ± 2.91	38.00 ± 1.79	50.30 ± 3.12	64.11 ± 3.81	7.78

Note: Data represent means ± SD (n = 3).
Abbreviations: NLCs, nanostructured lipid carriers; IC_{50}, half-maximal inhibitory concentration.

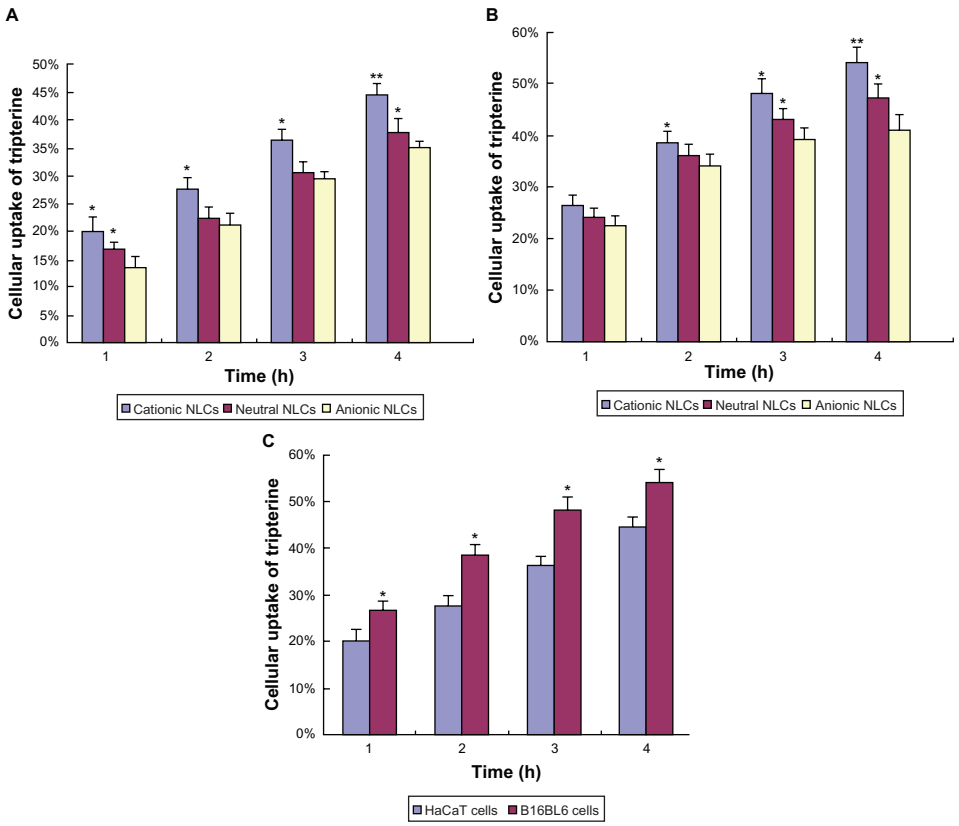

Figure 5 Cellular uptake of tripterine from the surface-charged nanostructured lipid carriers (NLCs). (**A**) HaCaT cells; (**B**) B16BL6 cells; (**C**) comparison of the uptake from cationic NLCs by HaCaT and B16BL6 cells.
Notes: Data represent means ± SD (n = 3); *$P < 0.05$ and **$P < 0.01$ versus the anionic NLCs in Figure 5A and B, and versus HaCaT cells in Figure 5C.

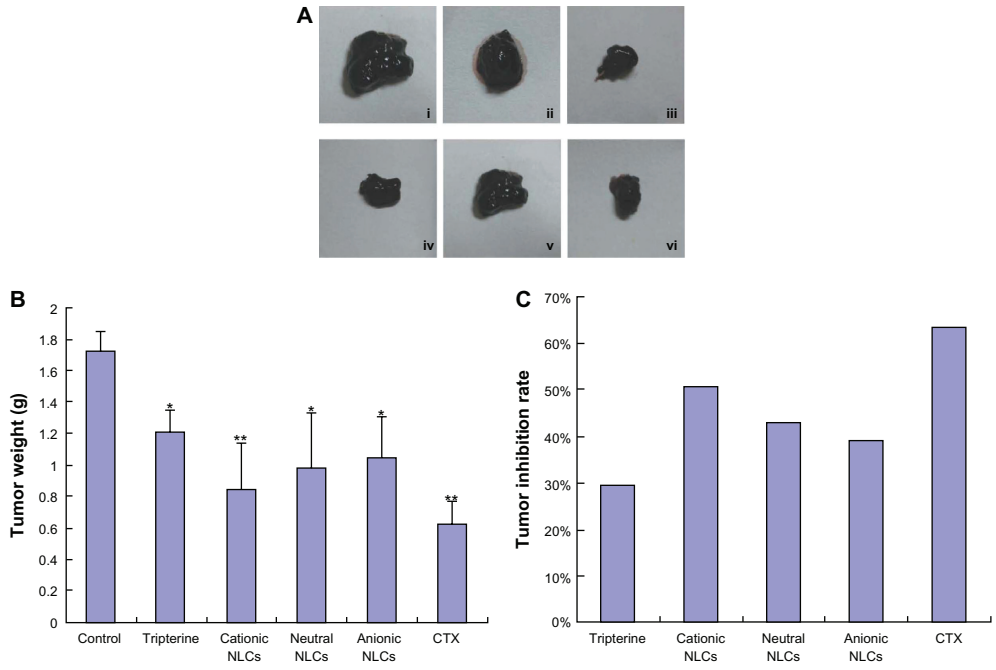

Figure 6 Effects of the surface-charged tripterine-loaded NLCs on tumor growth in vivo. (**A**) Representative images of tumors excised from C57BL/6 mice: (**i**) control (negative control); (**ii**) tripterine; (**iii**) cationic NLCs; (**iv**) neutral NLCs; (**v**) anionic NLCs; (**vi**) cyclophosphamide (CTX; 20 mg/kg intraperitoneally; positive control). In (**ii–v**), 6 mg/kg tripterine in 1% carbomer gel was used and the treatments were administered topically. (**B**) Tumor weight; (**C**) tumor inhibition rate after accounting for tumor weight.
Notes: Data represent means ± SD (n = 3); *$P < 0.05$ and **$P < 0.01$ versus the controls.
Abbreviation: NLCs, nanostructured lipid carriers.

antimelanoma efficacy of tripterine could be its poor water solubility and the physicochemical barrier formed by the skin. Therefore, the improved antimelanoma efficacy of tripterine in NLC formulations could be explained as follows. First, surface-charged NLCs can improve the solubility of tripterine, and their smaller particle size can enable efficient percutaneous penetration. The latter property also greatly increases the surface area of the particles and, thus, increases the contact area between the NLCs and the skin. Second, the mechanism of topical drug delivery is based on the mixing of the lipids from the particles and the skin surface. The NLCs composed of solid and liquid lipids, which have good biocompatibility, could increase drug delivery to the skin, thus achieving high antimelanoma efficacy.

As expected, the cationic NLCs displayed the highest tumor inhibition rates. This result also can be explained by their greater electrostatic interaction with the negatively charged skin surface and higher binding affinity toward B16BL6 cell surfaces, promoting drug permeation and antimelanoma efficacy.

Conclusion

The surface charges of NLCs have a great influence on the percutaneous penetration and anticancer efficacy of tripterine. Surface-charged tripterine-loaded NLCs, especially cationic ones, offer better antimelanoma efficacy than tripterine alone. Therefore, cationic NLCs are promising carriers of tripterine for topical antimelanoma therapy.

Acknowledgments

The authors report no conflicts of interest in this work. This work was supported by the Natural Science Foundation of Jiangsu Province (no SBK201022913) and Jiangsu Provincial Chinese Medicine Leading Talent Project (no LJ200913).

Disclosure

The authors report no conflicts of interest in this work.

References

1. Wissing SA, Kayser O, Müller RH. Solid lipid nanoparticles for parenteral drug delivery. *Adv Drug Deliv Rev*. 2004;56(9):1257–1272.
2. Müller RH, Radtke M, Wissing SA. Nanostructured lipid matrices for improved microencapsulation of drugs. *Int J Pharm*. 2002;242(1–2):121–128.
3. Müller RH, Radtke M, Wissing SA. Solid lipid nanoparticles (SLN) and nanostructured lipid carriers (NLC) in cosmetic and dermatological preparations. *Adv Drug Deliv Rev*. 2002;54(Suppl 1):S131–S155.
4. Küchler S, Radowski MR, Blaschke T, et al. Nanoparticles for skin penetration enhancement – a comparison of a dendritic core-multishell-nanotransporter and solid lipid nanoparticles. *Eur J Pharm Biopharm*. 2009;71(2):243–250.
5. Trommer H, Neubert RH. Overcoming the stratum corneum: the modulation of skin penetration. A review. *Skin Pharmacol Physiol*. 2006;19(2):106–121.
6. Gullett NP, Ruhul Amin AR, Bayraktar S, et al. Cancer prevention with natural compounds. *Semin Oncol*. 2010;37(3):258–281.
7. He MF, Liu L, Ge W, et al. Antiangiogenic activity of Tripterygium wilfordii and its terpenoids, *J. Ethnopharmacol*. 2009;121(1):61–68.
8. Kannaiyan R, Shanmugam MK, Sethi G. Molecular targets of celastrol derived from Thunder of God Vine: potential role in the treatment of inflammatory disorders and cancer. *Cancer Lett*. 2011;303(1):9–20.
9. Brinker AM, Ma J, Lipsky PE, Raskin I. Medicinal chemistry and pharmacology of genus Tripterygium (Celastraceae). *Phytochemistry*. 2007;68(6):732–766.
10. Salminen A, Lehtonen M, Paimela T, Kaarniranta K. Celastrol: Molecular targets of Thunder God Vine. *Biochem Biophys Res Commun*. 2010;394(3):439–442.
11. Yan C, Lei Z, Ling Y, Zhenhai Z, Qingqing W. Formulation, characterization and evaluation of the in vitro skin permeation of nanostructured lipid carriers encapsulated tripterine. International Symposium on Chemistry and Pharmaceutical Science; May 28–30, 2012; Macau China; In press 2012.
12. Manosroi A, Kongkaneramit L, Manosroi J. Stability and transdermal absorption of topical amphotericin B liposome formulations. *Int J Pharm*. 2004;270(1–2):279–286.
13. Song YK, Kim CK. Topical delivery of low-molecular-weight heparin with surface-charged flexible liposomes. *Biomaterials*. 2006;27(2):271–280.
14. Deshiikan SR, Papadopoulos KD. Modified booth equation for the calculation of zeta potential. *Colloid Polym Sci*. 1998;276:117–124.
15. Verma DD, Verma S, Blume G, Fahr A. Particle size of liposomes influences dermal delivery of substances into skin. *Int J Pharm*. 2003;258(1–2):141–151.
16. Vighi E, Ruozi B, Montanari M, Battini R, Leo E. Re-dispersible cationic solid lipid nanoparticles (SLNs) freeze-dried without cryoprotectors: characterization and ability to bind pEGFP-plasmid. *Eur J Pharm Biopharm*. 2007;67(2):320–328.
17. Feng L, Jia X, Zhu MM, Chen Y, Shi F. Antioxidant activities of total phenols of Prunella vulgaris L. in vitro and in tumor-bearing mice. *Molecules*. 2010;15(12):9145–9156.
18. Hu FQ, Jiang SP, Du YZ, Yuan H, Ye YQ, Zeng S. Preparation and characteristics of monostearin nanostructured lipid carriers. *Int J Pharm*. 2006;314(1): 83–89.
19. Han F, Li S, Yin R, Liu H, Xu L. Effect of surfactants on the formation and characterization of a new type of colloidal drug delivery system: nanostructured lipid carriers. *Colloids Surf A*. 2008;315(1–3):210–216.
20. Gonzalez-Mira E, Egea MA, Garcia ML, Souto EB. Design and ocular tolerance of flurbiprofen loaded ultrasound-engineered NLC. *Colloids Surf B Biointerfaces*. 2010;81(2):412–421.
21. Venkateswarlu V, Manjunath K. Preparation, characterization and in vitro release kinetics of clozapine solid lipid nanoparticles. *J Control Release*. 2004;95(3):627–638.
22. Patlolla RR, Desai PR, Belay K, Singh MS. Translocation of cell penetrating peptide engrafted nanoparticles across skin layers. *Biomaterials*. 2010;31(21):5598–5607.
23. Dragicevic-Curic N, Gräfe S, Gitter B, Winter S, Fahr A. Surface charged temoporfin-loaded flexible vesicles: in vitro skin penetration studies and stability. *Int J Pharm*. 2010;384(1–2):100–108.
24. Suwannateep N, Banlunara W, Wanichwecharungruang SP, Chiablaem K, Lirdprapamongkol K, Svasti J. Mucoadhesive curcumin nanospheres: biological activity, adhesion to stomach mucosa and release of curcumin into the circulation. *J Control Release*. 2011;151(2):176–182.
25. Herringson TP, Patlolla RR, Altin JG. Targeting of plasmid DNA-lipoplexes to cells with molecules anchored via a metal chelator lipid. *J Gene Med*. 2009;11(11):1048–1063.